
Monitoring of Therapy in Androgen-Dependent Prostate Tumor Model by Measuring Tumor Proliferation

Nobuyuki Oyama, MD, PhD^{1,2}; Datta E. Ponde, PhD¹; Carmen Dence, MS¹; Joonyoung Kim, PhD¹; Yuan-Chuan Tai, PhD¹; and Michael J. Welch, PhD^{1,2}

¹Mallinckrodt Institute of Radiology, Washington University School of Medicine, Saint Louis, Missouri; and ²Alvin J. Siteman Cancer Center, Washington University School of Medicine, Saint Louis, Missouri

3'-Deoxy-3'-¹⁸F-fluorothymidine (¹⁸F-FLT) has been recently described as a radiopharmaceutical for measuring cellular proliferation using PET imaging. Evaluation of tumor proliferative activity by PET using ¹⁸F-FLT could be a procedure to assess the viability of tumor, such as histologic grade, clinical stage, and prognosis as well as the early effects of cancer therapy. This study was undertaken to determine whether ¹⁸F-FLT is useful in the detection of prostate cancer as well as monitoring therapeutic effects in a human tumor model. **Methods:** The androgen-dependent human prostate tumor, CWR22, was implanted into athymic mice. This well-established model of prostate cancer was used in all studies. To determine the optimal imaging times for ¹⁸F-FLT, a biodistribution was performed in CWR22 mice. ¹⁸F-FLT (740 kBq [20 μ Ci]) was administered via the tail vein and uptake was determined in selected tissues at 5 min, 20 min, and 1, 2, and 4 h after injection ($n = 5$, each time point). Androgen ablation studies were conducted in the CWR22 model with either diethylstilbestrol (DES) or surgical castration. Animals received DES every 2 d for 3 wk. The effectiveness of therapy was monitored using ¹⁸F-FLT microPET as baseline, during treatment, and after treatment. Tracer accumulation in the tumor was then analyzed by comparing tumor-to-muscle ratios derived from reconstructed microPET data. **Results:** At 2 h after injection, the ¹⁸F-FLT uptake in tumor was 0.69 ± 0.14 percentage injected dose per gram of tissue, showing the highest activity of all organs measured. The microPET study with dynamic imaging showed that ¹⁸F-FLT uptake in blood reached its plateau within 1 min and was rapidly cleared, whereas ¹⁸F-FLT uptake in tumor reached its plateau in 30 min and remained up to 60 min. microPET using ¹⁸F-FLT successfully imaged the implanted CWR22 tumor in the mice at both 1 and 2 h after injection. There was a marked reduction of ¹⁸F-FLT uptake in tumor after castration or DES treatment; however, there were no differences in ¹⁸F-FLT uptake in the tumor in the control group. These changes of ¹⁸F-FLT uptake in tumor parallel the changes of actual tumor measurement. **Conclusion:** These results indicate that ¹⁸F-FLT is a useful tracer for detection of prostate cancer in an animal model. ¹⁸F-FLT has the

potential for monitoring the therapeutic effect of androgen ablation therapy in prostate cancer.

Key Words: PET; prostate cancer; tumor proliferation; 3'-deoxy-3'-¹⁸F-fluorothymidine

J Nucl Med 2004; 45:519–525

Androgen dependency is a characteristic behavior for many prostate cancers (1). Androgen ablation therapy has thus been used as the treatment for advanced disease, since chemotherapy has less therapeutic effect in prostate cancer than in other cancer types (2). A majority of those patients receiving androgen ablation therapy relapse within a few years, whereas others respond to therapy for extended periods. This varied response to the therapy indicates that there are large differences in the androgen dependency of prostate cancer patients. To achieve a greater response rate for patients with less androgen-dependent cancer, combination therapies with radiotherapy or chemotherapy are often explored. To select these patients, conventional imaging modalities such as ultrasonography and CT are used to monitor the effect of androgen ablation therapy. These prove to be less useful because these methods often need a few months of treatment for the first accurate assessment to be made. A more rapid evaluation method would allow androgen ablation therapy to be used only on patients who will respond to this mode of treatment.

PET for tumor imaging using the radiopharmaceutical ¹⁸F-FDG is a relatively new cancer imaging method that has been widely accepted as a highly effective means for imaging a wide variety of cancers. The success of ¹⁸F-FDG in many cancers has led to the evaluation of this radiopharmaceutical for use in prostate cancer. ¹⁸F-FDG was also evaluated for its usefulness in monitoring therapeutic effectiveness in prostate cancer in animal models (3) and in humans (4). These studies showed that the early change in glucose metabolism could enable monitoring metabolic changes in prostate tumors after treatment by imaging using ¹⁸F-FDG PET. However, ¹⁸F-FDG PET has a limitation in imaging

Received Mar. 25, 2003; revision accepted Oct. 23, 2003.
For correspondence or reprints contact: Michael J. Welch, PhD, Mallinckrodt Institute of Radiology, Washington University School of Medicine, Campus Box 8225, 510 South Kingshighway Blvd., St. Louis, MO 63110.
E-mail: Welchm@mir.wustl.edu

prostate cancer because of the relatively low performance of ^{18}F -FDG PET in detection of primary as well as distant disease (5–7).

Recently, 3'-deoxy-3'- ^{18}F -fluorothymidine (^{18}F -FLT) has been introduced as a proliferation radiopharmaceutical for PET imaging (8–10). Evaluation of tumor proliferative activity by PET using ^{18}F -FLT is a potential new procedure to assess the viability of tumor as well as the early effect of cancer therapy. In the current clinical study, ^{18}F -FLT uptake was higher in lung cancer tissue than that of benign masses, showing the usefulness of ^{18}F -FLT in differential diagnosis between malignant and benign tumors (11,12). However, to our knowledge, no report examining ^{18}F -FLT for prostate cancer has been published.

The purpose of this study is to evaluate the usefulness of ^{18}F -FLT to monitor the early therapeutic effects of androgen ablation therapy in prostate cancer using an animal tumor model and microPET imaging.

MATERIALS AND METHODS

Radiochemical Synthesis

^{18}F -Fluoride is produced via the $^{18}\text{O}(\text{p}, \text{n})^{18}\text{F}$ nuclear reaction by irradiating isotopically enriched ^{18}O -water with 15- to 16-MeV protons using either the Washington University Cyclotron Corporation CS-15 or the Japan Steel Works BC-16/8 medical cyclotron. Radioactivity emerging from the target was resin treated to reclaim the ^{18}O -water. ^{18}F -Fluoride was eluted from the resin in a solution of 0.02N potassium carbonate and used in subsequent reactions. ^{18}F -FLT was synthesized starting with anhydrothymidine, and microwave-mediated nucleophilic displacement by fluoride ion followed by acidic hydrolysis gave ^{18}F -FLT in just 60 min (13). The radiochemical yield was $12\% \pm 4\%$ (decay corrected) and radiochemical purity was $>99\%$.

Biodistribution Study

Animal experiments were conducted in compliance with the Guidelines for the Care and Use of Research Animals established by the Animal Studies Committee at our institution. Four- to 6-wk-old athymic *nu/nu* male mice were obtained from Charles River Laboratories. The CWR22 tumor line was a gift from Dr. Thomas G. Pretlow (Case Western Reserve University, Cleveland, OH). The CWR22 tumor was propagated in the animals by the implantation of minced tumor tissue, from a previously established tumor, into the subcutaneous tissue of the flanks of the mice. For the maintenance of high serum androgen levels, mice were implanted with 12.5 mg of 60-d-releasing testosterone pellets (Innovative Research of America) subcutaneously. Three weeks after tumor implantation, the mice were injected intravenously with 740 kBq (20 μCi) ^{18}F -FLT via tail vein. At the specified time points—5 min, 20 min, and 1, 2, and 4 h after injection—the animals were killed, samples of blood and tissue were excised and weighed, and the radioactivity was determined in a Beckman γ -8000 as previously reported (14). The injected doses were calculated from standards prepared from the injection solution, and the data are expressed as the percentage injected dose per gram of tissue (%ID/g).

microPET Imaging

Dynamic Scan. Approximately 6 wk after tumor implantation, CWR22 tumor-bearing mice were imaged in the prone position in

the microPET scanner (Concorde Microsystems). The mice were first anesthetized with 1%–2% isoflurane and placed near the center of the field of view (CFOV) of the microPET scanner where the highest image resolution and sensitivity are obtained. Dynamic imaging was performed for 60 min beginning at the injection of 18.5 MBq (500 μCi) ^{18}F -FLT into the mouse via a microcatheter (Harvard Apparatus, Inc.) placed in the external jugular vein. The image frame durations were as follows: 5 s per frame \times 24 frames, 10 s per frame \times 10 frames, 20 s per frame \times 10 frames, 150 s per frame \times 2 frames, 300 s per frame \times 4 frames.

Static Scan. CWR22 tumor-bearing mice were also analyzed with microPET to evaluate the change of FLT uptake in tumor during androgen ablation therapy. For the baseline PET scans, mice were first anesthetized with 1%–2% isoflurane and placed in the prone position in a custom-designed holder that allows simultaneous imaging of 2 mice. The entire holder was placed near the CFOV of the microPET scanner. A 10-min static scan was obtained 1 h after ^{18}F -FLT injection (18.5 MBq [500 μCi]). After baseline PET imaging, the mice were treated with surgical castration or dihydrotestosterone (DHT) every 2 d for 3 wk. Control mice had no treatment. On days 7, 14, and 21, microPET imaging was repeated with the same protocol as described for the baseline studies. At each microPET scan, the volume (cm^3) of implanted tumor was determined using the formula; $\frac{1}{2} \times$ longest diameter (length [cm]) \times shortest diameter (width [cm])². The methods of data collection and the reconstruction for microPET imaging have been described previously (4). Briefly, all raw data were first sorted into 3-dimensional sinograms, followed by Fourier rebinning and 2-dimensional filtered backprojection reconstruction using ramp filter cutoff at the Nyquist frequency. A region of interest (ROI) was placed on each tumor or other organs in the transaxial microPET images that include the entire tumor or organ volume. The average radioactivity concentration within a tumor or an organ was obtained from the average pixel values within the multiple ROI volume. From the ^{18}F -FLT dynamic study, time-activity curves were also calculated from the uptake index of the tumor, which was defined as the average radioactivity concentration divided by the total injected activity with the following formula:

$$\text{Uptake index} = \frac{\text{average radioactivity concentration in ROI (kBq}/\mu\text{L} [\mu\text{Ci}/\mu\text{L}])}{\text{injected dose (kBq} [\mu\text{Ci}])}$$

To eliminate the dependency on the injected activity, tumor-to-muscle ratios were used to compare the ^{18}F -FLT uptake in tumor before and after the treatment. In these microPET scans, the attenuation corrections were not applied since the accuracy of the measured attenuation correction was poor with this scanner, the amount of attenuation from a mouse body was relatively small, and the shape of a mouse body did not change significantly between different subjects; instead, the attenuation correction factors were incorporated into the system calibration. With the image reconstruction algorithm and filter described above, the resolution of this microPET system is between 2.0 and 3.0 mm full width at half maximum in each of the 3 dimensions within a 5-cm imaging field of view around the central axis of the tomograph. The partial-volume effect in estimating the ROI values from microPET images is small in these studies since the implanted tumors were >1 cm in diameter, which was well above the resolution limit of this system (15).

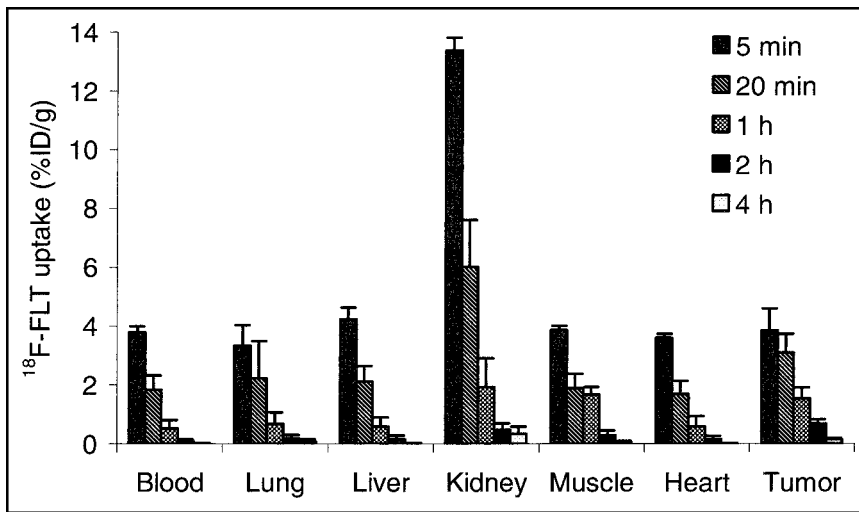


FIGURE 1. Biodistribution data show that ¹⁸F-FLT was rapidly cleared from the blood (3.79 %ID/g at 5 min, 0.53 %ID/g at 1 h). ¹⁸F-FLT uptake shows no large difference among the organs investigated at 5 and 20 min after injection, which mainly represents the blood flow of each organ. At 2 h after injection, the ¹⁸F-FLT uptake into tumor was 0.69 ± 0.14 %ID/g, showing the highest activity of all organs determined.

Statistical Evaluation

Biodistribution data are reported as the mean \pm the sample SD for %ID/g. The unpaired *t* test was used to compare tracer uptake before and after the treatments. Statistical significance was established at $P < 0.05$.

RESULTS

Biodistribution Study

Analysis of biodistribution data at 5 min, 10 min, and 1, 2, and 4 h was performed with ¹⁸F-FLT (Fig. 1). Biodistribution data showed that ¹⁸F-FLT was rapidly cleared from the blood (3.79 %ID/g at 5 min, 0.53 %ID/g at 1 h). ¹⁸F-FLT uptake showed no large difference among the organs investigated at 5 and 20 min after injection, which mainly represents the blood flow of each organ. At 2 h after injection,

the ¹⁸F-FLT uptake into tumor was 0.69 ± 0.14 %ID/g, showing the highest activity of all organs determined. This biodistribution study indicates that ¹⁸F-FLT is rapidly accumulated into tumor tissue and retained longer than in other tissues.

microPET Study

Dynamic Scan. Dynamic imaging was performed 0–60 min after ¹⁸F-FLT injection. ROIs were placed on the heart, muscle, and tumor at the left flank in the transaxial microPET images. A time–activity curve was generated from each ROI (Fig. 2). In the muscle, ¹⁸F-FLT uptake reached its plateau within a few minutes after injection, with approximately 60% of radioactivity remaining 30 min after injection. In the heart, ¹⁸F-FLT uptake reached its plateau within

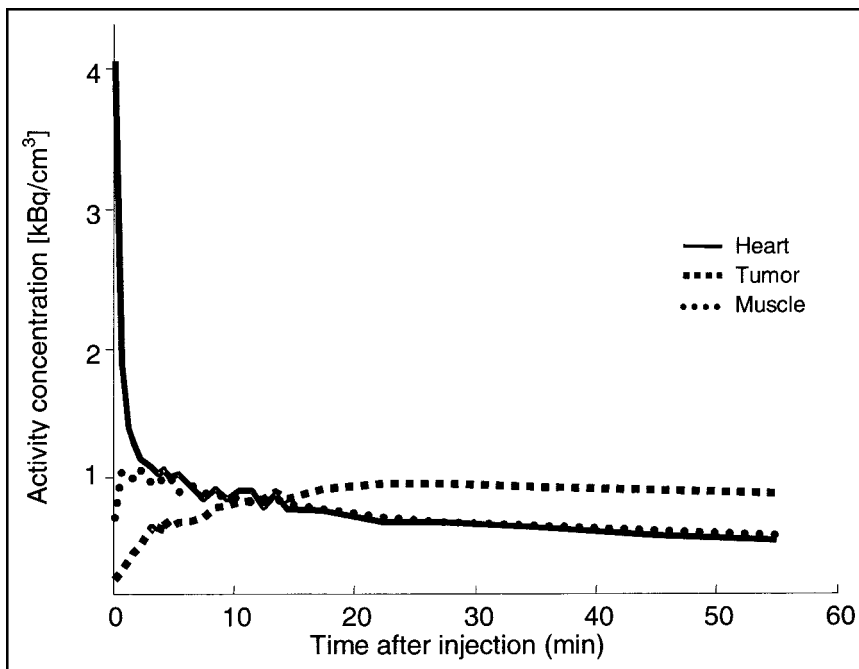
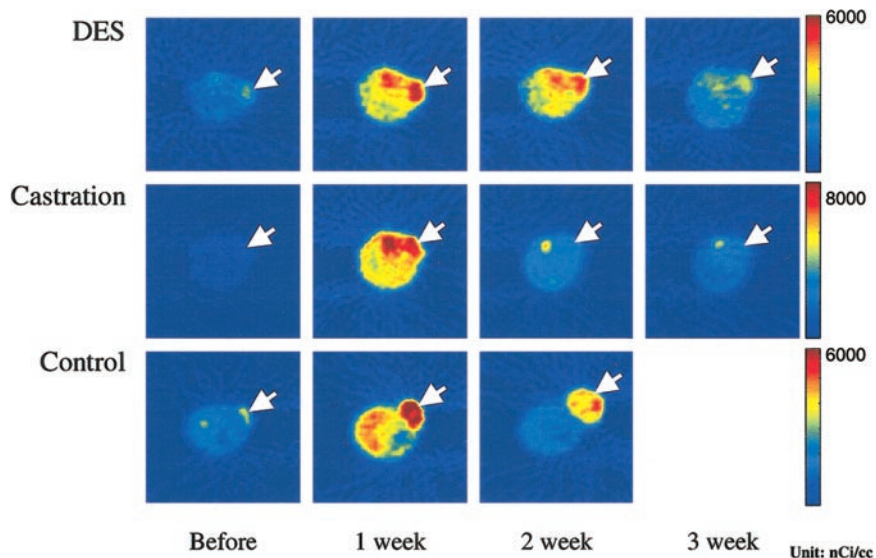


FIGURE 2. Time–activity curves for heart (—), muscle (●), and tumor (■) of CWR22 tumor-bearing mouse. ¹⁸F-FLT uptake into heart reached its plateau within 1 min, then it cleared very rapidly. ¹⁸F-FLT uptake in tumor reached its plateau in around 30 min, then it remained at least up to 60 min, showing slower clearance than muscle.

FIGURE 3. In this study, 3 wk after CWR22 tumor implantation, all mice were imaged in a microPET scanner (baseline scan). The mice were then divided into 3 groups: (a) treated with diethylstilbestrol (DES); (b) castrated after baseline PET scan; (c) control. All mice were scanned by ^{18}F -FLT microPET after 1, 2, and 3 wk after initiation of each treatment. The images show the transverse images of microPET for each group before and after treatment with the tumor identified by the arrow: (a) tumor stopped growing after DES treatment; (b) tumor size decreased after castration; (c) the tumor kept growing. By week 3, all control mice were euthanized following institutional regulations on tumor burden.



1 min after injection, with rapid clearance during the next 10 min. In the tumor, it took approximately 20 min to reach its plateau for ^{18}F -FLT, with 90% of radioactivity remaining 60 min after injection. After analysis of the data by the ROI and time-activity curve, it was evident that a static image 30 min after injection supplied images and data of sufficient contrast for future studies.

Static Scan. Coronal microPET images using ^{18}F -FLT clearly demonstrated tumors implanted in the left flank of the mice (Fig. 3). Static images 1 and 2 h after injection were reconstructed, and ROIs were placed on lumbar muscle and tumor using the same transverse images. ^{18}F -FLT uptake was compared in the same mice before and 1, 2, and 3 h after the treatment using tumor-to-muscle ratios. By 2 wk, 2 mice of the control group were euthanized following our institutional regulations on tumor burden. Another 2 mice were also killed by 3 wk for the same reason; there-

fore, no control mice were imaged at 3 wk. The results are shown in Figures 4 and 5. At 1 h after injection, tumor-to-muscle ratios in the control mice group were 2.50 ± 0.61 at baseline, 2.30 ± 0.75 at 1 wk, and 2.62 ± 0.75 at 2 wk, showing no large difference during the 2-wk observation. On the other hand, tumor-to-muscle ratios in the diethylstilbestrol (DES) group mice were 3.55 ± 0.59 at baseline, 1.31 ± 0.29 at 1 wk, 1.49 ± 0.33 at 2 wk, and 1.61 ± 0.49 at 3 wk; in the castration group mice, the ratios were 2.52 ± 0.21 at baseline, 0.87 ± 0.29 at 1 wk, 1.00 ± 0.20 at 2 wk, and 1.00 ± 0.13 at 3 wk, which demonstrated a significant decrease of ^{18}F -FLT uptake in tumor 1 wk after the androgen ablation therapy (DES, $P = 0.01$; castration, $P = 0.01$; unpaired t test). At 2 h after injection images, tumor-to-muscle ratios in the control mice group were 3.95 ± 1.00 at baseline, 5.27 ± 1.79 at 1 wk, and 3.24 ± 2.00 at 2 wk. Tumor-to-muscle ratios in the DES-treated mice group were 4.27 ± 1.51 at

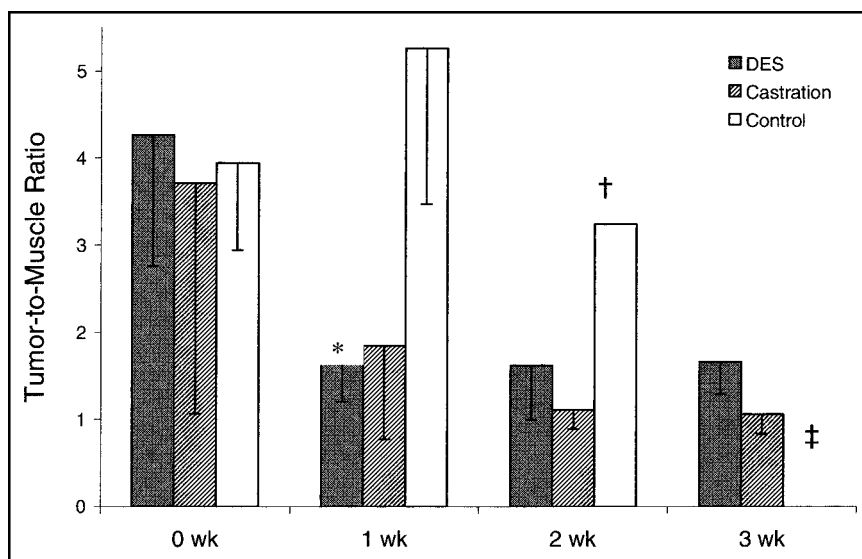


FIGURE 4. At 1 h after injection, ^{18}F -FLT uptake in tumor decreased after initiation of diethylstilbestrol (DES) or castration. There were no large differences in ^{18}F -FLT uptake in the control group († 2 mice survived; ‡ no mice survived).

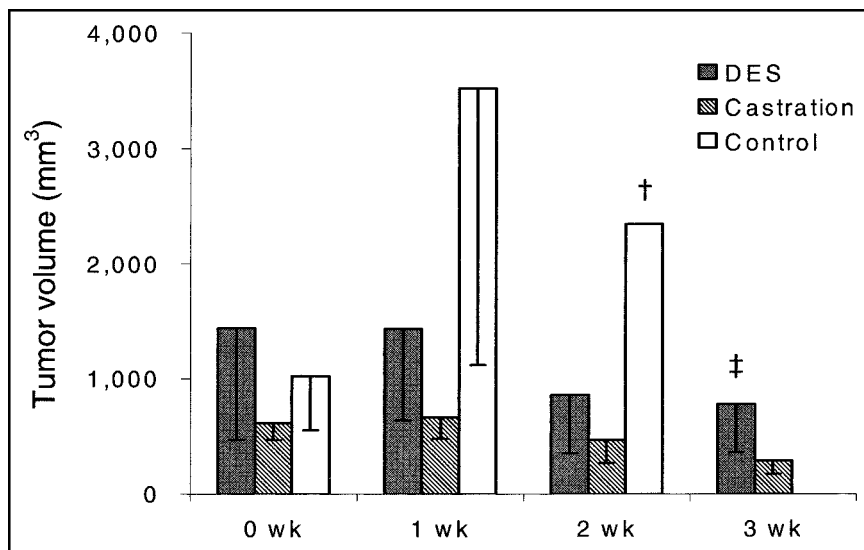


FIGURE 5. The changes of actual tumor volume seem to be well correlated with the change of ^{18}F -FLT uptake in tumor in each group (†2 mice survived; ‡no mice survived).

baseline, 1.65 ± 0.45 at 1 wk, 1.62 ± 0.63 at 2 wk, and 1.66 ± 0.36 at 3 wk ($P = 0.03$, unpaired t test, between baseline and 0 wk); in the castration mice group, the ratios were 3.71 ± 2.65 at baseline, 1.84 ± 1.07 at 1 wk, 1.11 ± 0.21 at 2 wk, and 1.06 ± 0.23 at 3 wk. The tumor volume of each mouse was also measured. The tumor volume of control mice kept increasing after a baseline scan, whereas the tumor volume of treated mice decreased after initiation of the androgen ablation therapy.

DISCUSSION

It is essential for successful prostate cancer treatment to monitor the tumor growth in the early phase of androgen ablation therapy, since this is the preferable way to distinguish between patients with prostate cancers who show poor prognosis and those who show better prognosis. In the last 2 decades, the serum prostate-specific antigen (PSA) has been used for this purpose. The LH-RH (luteinizing hormone-releasing hormone) agonist is the most popular agent for androgen ablation therapy for advanced prostate cancer disease, which leads to suppression of LH and of testosterone production equivalent to levels obtained by castration. However, this peptide stimulates LH release, causing an initial flare of serum testosterone during the first 2–3 wk associated with a rise in serum PSA, followed by a relatively slow serum PSA decrease. Therefore, measurement of serum PSA only allows the first accurate assessment of androgen ablation therapy after a few months of therapy initiation.

^{18}F -FDG PET has changed the ability to diagnose malignant tumors. It has been shown that ^{18}F -FDG PET is useful to detect many kinds of cancers because of consumption of large amounts of glucose as an energy source. Evaluation of tumor metabolism by PET is a relatively new procedure for assessing the early effects for cancer therapy and has already been applied to breast cancer (16). Recently, ^{18}F -FDG

PET has shown its value in demonstrating prostate cancer metabolism in animal models as well as in humans. In a human study it has been reported that ^{18}F -FDG uptake in prostate cancers was suppressed by androgen ablation after 1–3 mo (3). In another report, an animal study was conducted to determine whether PET imaging using ^{18}F -FDG and ^{11}C -acetate could evaluate early metabolic changes in prostate cancer after androgen ablation in an animal model (4). The androgen-dependent tumor-bearing mice were treated with either surgical castration or DES, and a biodistribution study and microPET imaging were performed before and after the treatment. One week of DES treatment caused a decrease in ^{18}F -FDG uptake in the tumor but not in ^{11}C -acetate uptake. According to this report, the early metabolic changes could enable monitoring metabolic changes in prostate cancer after treatment by imaging using ^{18}F -FDG PET. Although these reports have shown the efficacy of ^{18}F -FDG PET imaging for monitoring anticancer therapy effect in prostate cancer, the problem with ^{18}F -FDG PET imaging is its relatively low sensitivity and specificity in prostate cancer because of low glucose utilization due to its slow growth, with most reports showing a range of 50%–70% for both measures (5–7).

Recently, ^{18}F -FLT has been proposed as a new PET tracer for cell proliferation (8). By evaluating proliferative activity of tumor, PET using ^{18}F -FLT may enable assessment of the viability of the tumor as well as the early effect of cancer therapy. ^{18}F -FLT is an analog of thymidine; when it enters the body, it is taken up by cells and accumulates after being phosphorylated by thymidine kinase 1 (TK1). It is not incorporated into DNA but is retained in the cell without being metabolized. TK1 activity is high in proliferating cells, and it is regulated by S-phase expression of the cells. Indeed, ^{18}F -FLT uptake is found to be well correlated with TK1 activity and the percentage of the S-phase cell fraction (10,17). Being accumulated in highly proliferative cells,

^{18}F -FLT PET enables measurement of the cellular TK1 activity, which is closely related to cellular proliferation.

The biodistribution study showed that the ^{18}F -FLT uptake was highest in the kidney up to 1 h, which demonstrates that most of the ^{18}F -FLT is excreted into urine via the kidney. At 2 h after injection, tumor tissue showed the highest ^{18}F -FLT uptake of all organs. This biodistribution study indicates that 2 h after injection is a potential ideal time point to delineate prostate cancer tissue using an ^{18}F -FLT PET scan with the highest contrast to muscle and the other organs. CWR22 prostate cancer tissues implanted into 12 mice were well delineated with adequate tumor background contrast using microPET at 2 h after injection. This study shows that ^{18}F -FLT PET has a potential to detect prostate cancer tissue with high sensitivity. We did not scan another prostate cancer tumor other than CWR22 in this study. Further animal studies using another type of prostate cancer tumor model and different scanning time points as well as human studies are needed to determine the general sensitivity of ^{18}F -FLT PET for prostate cancer.

The second purpose of this study was to investigate the potential of ^{18}F -FLT PET in monitoring an early therapeutic effect of androgen ablation therapy for prostate cancer in an animal model. Dittmann et al. examined the usefulness of ^{18}F -FLT PET for monitoring the early effects of anticancer chemotherapy on tumor cell proliferation using OSC-1, an esophageal squamous cell carcinoma, in vitro (9). After incubation of OSC-1 cells with chemotherapy agents for certain periods of time, the cells were incubated with normal culture media and ^{18}F -FLT uptake into tumor cells was determined. ^{18}F -FLT uptake was significantly decreased at cytostatic concentrations of cisplatin. This finding shows that ^{18}F -FLT uptake in tumor is a promising predictor of tumor cell proliferation in the early phase of cancer therapy. With regard to the correlation of ^{18}F -FLT uptake with proliferation parameters, Vesselle et al. reported a strong correlation between ^{18}F -FLT uptake into human lung cancer and the Ki-67 score or the percentage of S-phase fraction (12). In the current study, the microPET images showed that androgen ablation caused a decrease of ^{18}F -FLT uptake in the androgen-dependent tumor, whereas there was no significant difference in control mice. These findings may indicate that the decrease of serum testosterone level due to DES therapy or castration influences TK1 activity. TK1 activity evaluated with ^{18}F -FLT uptake is shown to be well correlated with the actual proliferative activity of the cells (10), although some discrepancy between TK1 activity and proliferation has been reported (18). According to the study of Agus et al., the androgen withdrawal results in cell arrest of CWR22 prostate tumor before changes to apoptosis (19). With the result of this study, ^{18}F -FLT PET appears to be useful as a marker of proliferation and hormone therapy monitoring.

Many patients with advanced prostate cancer disease have osseous metastases. Evaluation of tumor proliferation activity at the bone metastatic lesion is important in moni-

toring tumor response to anticancer therapy. However, there is an intense FLT uptake present in bone marrow, which has a potential to be difficult in evaluation of bone disease. Further study is needed to determine the usefulness of FLT PET imaging for osseous metastatic disease.

^{18}F -FLT is a possible tracer for evaluation of changes in prostate tumor metabolism, and it will contribute to predict androgen dependency of prostate cancer in the early phase of androgen ablation therapy. Further studies are required to clarify the relationship between the changes of ^{18}F -FLT uptake and cellular proliferation markers after initiation of androgen ablation therapy using androgen-dependent and independent prostate cancer tumors.

CONCLUSION

These results confirm that microPET using ^{18}F -FLT showed a clear delineation of the implanted prostate tumor. ^{18}F -FLT is a possible tracer to evaluate changes in the proliferation activity of prostate cancer during androgen ablation therapy. The investigation of proliferation activity may be able to predict the androgen dependency of prostate cancer in the early phases of androgen ablation therapy. These results will likely lead to human trials in the near future.

ACKNOWLEDGMENTS

This study is supported by a grant from the U.S. Department of Energy (grant DOE DE-FG02-84ER-60218). The microPET imaging was supported by a National Institutes of Health/National Cancer Institute (NCI) Small Animal Imaging Resource Program grant (1 R24 CA83060). We thank the Small Animal Imaging Core of the Alvin J. Siteman Cancer Center at Washington University and Barnes-Jewish Hospital in St. Louis, Missouri, for additional support of the microPET imaging. The Core is supported by an NCI Cancer Center Support grant (1 P30 CA91842). We also thank Lori A. Strong, Jerrel R. Rutlin, Nicole M. Fettig, John A. Engelbach, Lynne A. Jones, and Terry L. Sharp for their technical support in the biodistribution study and microPET imaging and Sally W. Schwarz for the production of isotopes. A preliminary report of this work was presented at the 49th Annual Meeting of the Society of Nuclear Medicine in Los Angeles, CA, June 15–19, 2002 (20).

REFERENCES

1. Huggins C, Hodges CV. Studies on prostate cancer. I. The effect of estrogen and of androgen injection on serum phosphatases in metastatic carcinoma of the prostate. *Cancer Res.* 1941;1:293–297.
2. Eisenberger MA. Chemotherapy for prostate carcinoma. *NCI Monogr.* 1988;7:151–163.
3. Oyama N, Akino H, Suzuki H, et al. FDG PET for evaluating the change of glucose metabolism in prostate cancer after androgen ablation. *Nucl Med Commun.* 2001;22:963–969.
4. Oyama N, Kim J, Jones LA, et al. MicroPET assessment of androgenic control of glucose and acetate uptake in the rat prostate and a prostate cancer tumor model. *Nucl Med Biol.* 2002;29:783–790.
5. Effert PJ, Bares R, Handt S, Wolff JM, Bull D, Jakes G. Metabolic imaging of

- untreated prostate cancer by positron emission tomography with 18-fluorine-labeled deoxyglucose. *J Urol*. 1996;155:994–998.
6. Oyama N, Akino H, Suzuki Y, et al. The increased accumulation of [¹⁸F]fluoro-deoxyglucose in untreated prostate cancer. *Jpn J Clin Oncol*. 1999;29:623–629.
 7. Shreve PD, Grossmann HB, Gross MD, Wahl RL. Metastatic prostate cancer: initial findings of PET with 2-deoxy-2-[¹⁸F]fluoro-D-glucose. *Radiology*. 1996;199:751–756.
 8. Shields AF, Grierson JR, Dohmen BM, et al. Imaging proliferation in vivo with [F-18]FLT and positron emission tomography. *Nat Med*. 1998;4:1334–1336.
 9. Dittmann H, Dohmen BM, Kehlach R, et al. Early change in [¹⁸F]FLT uptake after chemotherapy: an experimental study. *Eur J Nucl Med*. 2002;29:1462–1469.
 10. Rasey JS, Grierson JR, Wiens LW, Kolb PD, Schwartz JL. Validation of FLT uptake as a measure of thymidine kinase-1 activity in A549 carcinoma cells. *J Nucl Med*. 2002;43:1210–1217.
 11. Buck AK, Schirmmeister H, Hetzel M, et al. 3-Deoxy-3-[¹⁸F]fluorothymidine-positron emission tomography for noninvasive assessment of proliferation in pulmonary nodules. *Cancer Res*. 2002;62:3331–3334.
 12. Vesselle H, Grierson J, Muzi M, et al. In vivo validation of 3'-deoxy-3'-[¹⁸F]fluorothymidine ([¹⁸F]FLT) as a proliferation imaging tracer in humans: correlation of [¹⁸F]FLT uptake by positron emission tomography with Ki-67 immunohistochemistry and flow cytometry in human lung tumors. *Clin Cancer Res*. 2002;8:3315–3323.
 13. Ponde DE, Oyama N, Welch MJ, McCarthy TJ. Synthesis of fluorothymidine ([¹⁸F]FLT) for radiotracer of tumors [abstract]. *Abstr Pap AM Chem Soc*. 2002;223:081-Nucl Part 2.
 14. Kiesewetter DO, Kilbourn MR, Landvatter SW, Heiman DF, Katzenellenbogen JA, Welch MJ. Preparation of tumor fluorine-18-labeled estrogens and their selective uptake in target tissues of immature rats. *J Nucl Med*. 1984;25:1212–1221.
 15. Tai YC, Chatziioannou A, Siegel S, et al. Performance evaluation of the micro-PET P4: a PET system dedicated to animal imaging. *Phys Med Biol*. 2001;46:1845–1862.
 16. Dehdashti F, Mortimer JE, Siegel BA, et al. Positron tomographic assessment of estrogen receptors in breast cancer: comparison with FDG-PET and in vitro receptor assays. *J Nucl Med*. 1995;36:1766–1774.
 17. Toyohara J, Waki A, Takamatsu S, Yonekura Y, Magata Y, Fujibayashi Y. Basis of FLT as a cell proliferation marker: comparative uptake studies with [³H]thymidine and [³H]arabinothymidine, and cell-analysis in 22 asynchronously growing tumor cell lines. *Nucl Med Biol*. 2002;29:281–287.
 18. Toyohara J, Kato-Azuma M, Waki A, et al. Basis of FLT as a cell proliferation marker: comparative uptake studies with thymidine, arabinothymidine and FDG, and cell-analysis in 22 asynchronously growing tumor cell lines [abstract]. *J Nucl Med*. 2001;42(suppl):83P.
 19. Agus DB, Cordon-Cardo C, Fox W, et al. Prostate cancer cell cycle regulators: response to androgen withdrawal and development of androgen independence. *J Natl Cancer Inst*. 1999;91:1869–1876.
 20. Oyama N, Ponde DE, Kim JY, et al. MicroPET imaging of prostate cancer using ¹⁸F-FLT: androgen dependent tumor model study [abstract]. *J Nucl Med*. 2002;43(suppl):27P.

